Received: *July 13, 2001*, Accepted: *August 13, 2001*

On the strong-coupling spectrum of pure SU(3) Seiberg-Witten theory

Brett J. Taylor

Department of Physics, University of Wales Swansea
Swansea, SA2 8PP, UK
E-mail: pybr@swansea.ac.uk

Abstract: We consider the two complex dimensional moduli space of supersymmetric vacua for low energy effective $\mathcal{N} = 2$ SYM with gauge group SU(3). We describe, at the topological level, a consistent model of how the relevant curves of marginal stability (CMS) intertwine with the branch cuts to partition the moduli space into pieces carrying different BPS spectra. At strong coupling we find connected *cores* which carry a smaller BPS spectrum than that at weak coupling. At the strongest coupling we find *double cores* which carry a finite BPS spectrum. These include not only states one can deduce from the monodromy group, but three states, bounded away from weak coupling, each of which we interpret as a bound state of two BPS gauge bosons. We find new BPS states at weak coupling corresponding to a excitations of a state with magnetic charge a simple co-root, with respect to the other simple root direction.

Keywords: Nonperturbative Effects, Solitons Monopoles and Instantons, Supersymmetric Effective Theories.

JHEP08(2001)031

Contents

1. Introduction

The pioneering work of Seiberg and Witten [1, 2] gave exact non-perturbative results for wilsonian low energy effective $\mathcal{N} = 2$ supersymmetric gauge theory in the case of gauge group SU(2) and with 0, 1, 2, 3 and 4 hypermultiplets in the fundamental representation. Many hints were given as to how this could be extended to higher gauge groups or in other directions. These were quickly seized upon and fleshed out in some detail by many groups [10],[22]–[30].

Generic to all the SU(2) models seemed to be the existence of a *core* region at strong coupling, bounded from the weakly coupled region by a curve of marginal stability (CMS) whereupon hitherto stable BPS states become marginally stable and decay into two (lighter) elements of a reduced spectrum which lies within the core.

Seiberg and Witten did not pursue the calculation to find the position of the CMS, leaving us to wait for the rigorous analysis of Bilal and Ferrari [3, 4, 5]. Rather, they contented themselves with an argument for its existence based on the consistency of the weakly coupled BPS spectrum. Only three states in this spectrum transform through the quantum branch cut back into another state of the spectrum (another one of the three). They argue that a CMS must be present surrounding this branch cut whereupon all the other states in the weak-coupling spectrum decay to the favoured three.

In this paper we shall attempt a similar argument for the SU(3) moduli space. We first consider the case of weak coupling. We then present a consistent example of how this may be continued to when an SU(2) subalgebra corresponding to a root direction becomes strongly coupled, and finally to when two such subalgebras have strong coupling.

An initial inspection would conclude that the BPS spectrum at weak coupling consists not of just one tower of dyons, but of three. There are many additional complications, one of which, described in [7] by Hollowood and Fraser, being that there are disconnected regions of moduli space at weak coupling carrying different towers of BPS dyons, separated at both weak and strong coupling by a combination of branch cuts and curves of marginal stability. However, for gauge groups of rank greater than one, such as in this case, the two Higgs fields are generically non-aligned in group space. It has been shown [12] that in this instance many more BPS towers exist at weak coupling, indeed a countably infinite number. All except the previously mentioned three of these exist as higher spin multiplets, and are labelled by an integer m which is twice the spin of the highest spin state in the multiplet. We find that as we increase the strength of the coupling these decay on curves of marginal stability into smaller multiplets until we reach a region where we are left with the three tower situation found in [7, 8, 9].

We shall find curves which exist only at strong coupling, as well as ones which stretch to and can be extrapolated from weak coupling. When only one of the sub-SU(2)'s is strong, there is a three-dimensional bounded region, called the core, containing a reduced BPS spectrum analogous to the SU(2) case. Within self-intersections of this space lie disconnected bounded regions with a further reduced spectrum (double cores) which correspond to the case when the sub-SU(2)'s of two roots are strongly coupled. Created at the double cores, but spreading throughout the strongly-coupled region we find the existence of three states P_i with no magnetic charge, and electric charge equal to the difference of two roots (counting $-(\alpha_1+\alpha_2)$ as the third root). We interpret these as bound states of massive gauge bosons.

This model predicts the existence of more new towers at weak coupling which we believe to have been overlooked. These can be created by passing already discovered higher spin multiplets through branch cuts with classical monodromies. This creates states which, like the ones found in [12], have electric charges which together fill out half the root lattice at any particular point, but have simple co-roots as magnetic charge. We are thus led to speculate that dyons with simple co-root magnetic charges at weak coupling, like those with non-simple co-roots, have low energy dynamics determined by supersymmetric quantum mechanics on a hyperkähler space of more than four real dimensions. Exciting momenta in one of the new directions corresponds to a sort of Witten effect involving a charge non-proportional to the magnetic one. This is somehow restricted to the more usual subspace $\mathbb{R}^3 \times S^1$, most probably due to the potential from a triholomorphic Killing vector field on the relative moduli space blowing up when the two Higgs fields happen to align.

Interestingly the mechanism can be seen explicitly at strong coupling, where states with these charges are created when one repeatedly wraps the normal simple root states about the core where the other simple root direction is strongly coupled. More than that, the charge picked up upon each rotation is that of the gauge boson bound states P_i, which exist at, and only at, strong coupling. In this core it seems one is allowed to excite in this novel direction, but curves of marginal stability restrict the spectrum to only zero and one units in the proportional direction, as for the SU(2) case.

We shall choose to slice up our four-dimensional space into concentric three spheres as suggested by Argyres and Douglas [11], and to study the picture at various generic radii. We begin with large radius which corresponds to weak coupling, and then steadily decrease the radius until we have mapped out the entire space.

2. The perturbative weak-coupling BPS spectra

Seiberg-Witten theory is a wilsonian low-energy effective theory that is perturbatively 1-loop exact, and non-perturbatively affected by a series of instanton corrections. In $\mathcal{N}=1$ language

$$\mathcal{L}_{\text{eff}} = \frac{1}{4\pi}\,\text{Im}\left[\int d^4\theta \frac{\partial \mathcal{F}(A)}{\partial A}\bar{A} + \int d^2\theta \frac{1}{2}\frac{\partial^2 \mathcal{F}(A)}{\partial A^2} W^\alpha W_\alpha\right],$$

where $\mathcal{F}$ is the holomorphic prepotential. The $\mathcal{N}=2$ vector supermultiplet has two $\mathcal{N}=1$ components, A being the chiral one, whose lowest component is a, and V the vector one. $W_\alpha = -\frac{1}{4}\bar{D}^2 D_\alpha V$ is the abelian field strength supermultiplet. We can split $\mathcal{F}$ into its constituent pieces

$$\mathcal{F} = \mathcal{F}_{1-\text{loop}} + \sum_{n=1}^{\infty} \mathcal{F}_n \left(\frac{\Lambda}{a}\right)^{\kappa n}.$$

At weak coupling the instantons are exponentially suppressed so we may concentrate on the perturbative analysis.

If we find $a_D = \partial\mathcal{F}/\partial a$ then it is a simple matter to integrate to find $\mathcal{F}$. For SU(N) broken to U(1)$^{N-1}$ one finds a sum over positive roots:

$$a_D = \frac{i}{2\pi}\sum_{\alpha_i \in \Phi^+} \alpha_i(\alpha_i.a)\left[1 + \ln\left(\frac{\alpha_i.a}{\Lambda}\right)^2\right].$$

One can read from this that the weak-coupling limit occurs when $|a.\alpha_i| \gg 0$ for all the roots α_i. This is essentially the large a limit, but excluding points close to fundamental weight directions. When $|a.\alpha_i| = 0$ the gauge group is not generically broken, a non-abelian subgroup reappears, the extra massless particles alter the effective theory, and this is realized as a singularity where the previous theory breaks down. For SU(3) the weakly coupled regions are sketched in figure 1. We label α_3 as lying between the other two roots (or $-\alpha_2$ between $-\alpha_3$ and α_1, or $-\alpha_1$ between $-\alpha_3$ and α_2).

In [7] Hollowood and Fraser consider the spectrum of BPS states for the weakly coupled region with the two Higgs fields aligned in group space. For points which lie within the fundamental Weyl chamber chosen such that α_1 and α_2 are the simple roots, they find that the weakly-coupled space is split into two domains, each with a slightly different spectrum. Corresponding to each of the two simple root directions there exists a tower of dyons with magnetic charge equal to the co-root in question, and electrically charged with an integer multiple of the same root.

$$Q_1^n = (\alpha_1, (n-1)\alpha_1)\,; \qquad Q_2^n = (\alpha_2, n\alpha_2)\,.$$

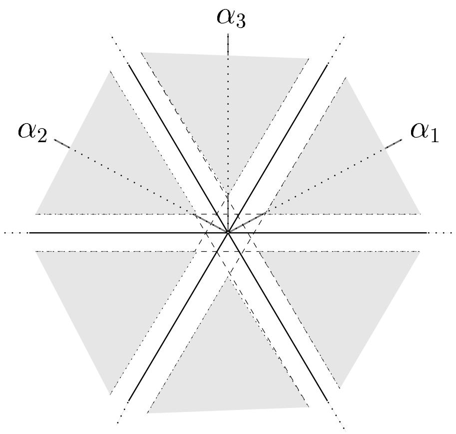

Figure 1: Using a as a coordinate the moduli space lives in the complexified Cartan subalgebra of SU(3). Shaded here are the weakly coupled regions, those bounded away from the weight directions. They extend off to infinity.

For a non-simple root it was shown in [12] using analysis in [31] that nowhere at weak coupling does a similar situation occur for α_3 with electric charge proportional to magnetic charge. Rather, the electric charge, which still remains in the root lattice, is shifted, equally for every state in the tower, in the direction of one of the other roots. There are two possiblilities:

$$Q_{3-}^n = (\alpha_3, -\alpha_1 + n\alpha_3)\,; \qquad Q_{3+}^n = (\alpha_3, +\alpha_1 + n\alpha_3)\,.$$

Between them lies the barrier of a curve of marginal stability (CMS) which partitions the space in two. Note that if a BPS state is present, so is its antimatter partner with the opposite charges, and therefore we shall ignore any overall minus signs in the charge vectors.

We now choose to parametrize the moduli space in terms of the Casimirs

$$u = \langle \mathrm{tr}(\phi^2) \rangle\,; \qquad v = \langle \mathrm{tr}(\phi^3) \rangle\,.$$

Following Argyres and Douglas [11], we foliate the space by hypersurfaces with the topology of three-spheres,

$$4|u|^3 + 27|v|^2 = R^6\,,$$

and study the three-space produced upon stereographic projection of each of these slices — i.e. by the map

$$(\operatorname{Re} u, \operatorname{Im} u, \operatorname{Re} v, \operatorname{Im} v) \to \left(\frac{\operatorname{Re} u}{R^3 - \sqrt{27}\operatorname{Im} v}, \frac{\operatorname{Im} u}{R^3 - \sqrt{27}\operatorname{Im} v}, \frac{\operatorname{Re} v}{R^3 - \sqrt{27}\operatorname{Im} v}\right).$$

The three-spheres have been chosen such that the intersection of the surface of singularities with a large three sphere is a closed curve in the form of a knot, the *trefoil* which wraps thrice around an auxilliary torus in one direction as it wraps twice around the other cycle.

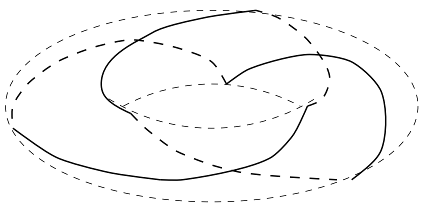

Figure 2: The classical trefoil $\mathcal{T}_{cl}$ wrapping three times around one cycle as it wraps twice around the other.

The large R limit corresponds to the large a limit, and so contains the weak-coupling limit when far from a singularity. In our picture this corresponds either to the point at infinity or at the origin. Together with gauge bosons W_1, W_2 and W_3, the set $\{Q_1^n, Q_2^n, Q_{3-}^n\}$ is the massive BPS spectrum around infinity, and $\{Q_1^n, Q_2^n, Q_{3+}^n\}$ that near the origin.

As can be seen from the perturbative formula for a_D, upon traversing a small loop around the singular surface, a and a_D mix. This is an example of monodromy. One can realize this by the strategic placement of branch cuts emanating from the singular surface. Associated to each cut is a matrix with integer entries which performs the mixing between a and a_D (and any other global U(1) charges present). The mass of a BPS state with (magnetic, electric) charge (g, q) is given by the modulus of a central charge $Z = g.a_D - q.a$, hence one can see that mondromy can also be realised by acting on the charges (g, q) by the inverse of the monodromy matrix. Following [10] we choose to use the basis (Dynkin, fundamental) for our charges, in which $(\alpha_1, 0) = (1, 0, 0, 0)$, $(\alpha_2, 0) = (0, 1, 0, 0)$, $(0, \alpha_1) = (0, 0, 2, -1)$, and $(0, \alpha_2) = (0, 0, -1, 2)$. The monodromy matrices form a group, a subgroup of $\mathrm{Sp}(2(N-1), \mathbb{Z})$.

The branch cuts must be of real-codimension one, so will have sections on our three-sphere that form a (self-intersecting) surface. The only two choices consistent with the monodromy group are the ruled surfaces formed as the locus swept out by lines connecting each point on the trefoil to either a point near the origin, or to a point near infinity (or, of course, by adding any number of non-topology changing perturbations to this). We choose to pick our cuts all meeting at the origin. Our first choice is then to include the following three mondromy matrices given in [10] as in figure 3.

$$N_1 = \begin{pmatrix} -1 & 0 & 4 & -2 \\ 1 & 1 & -2 & 1 \\ 0 & 0 & -1 & 1 \\ 0 & 0 & 0 & 1 \end{pmatrix}; \qquad N_2 = \begin{pmatrix} 1 & 1 & 1 & -2 \\ 0 & -1 & -2 & 4 \\ 0 & 0 & 1 & 0 \\ 0 & 0 & 1 & -1 \end{pmatrix};$$

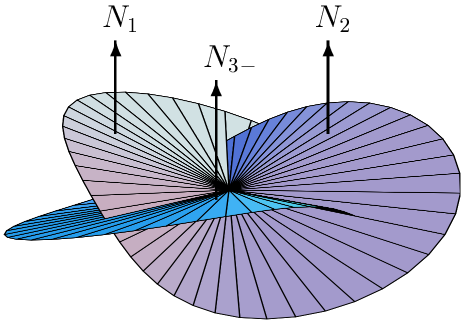

Figure 3: The classical branch cuts form a self-intersecting surface.

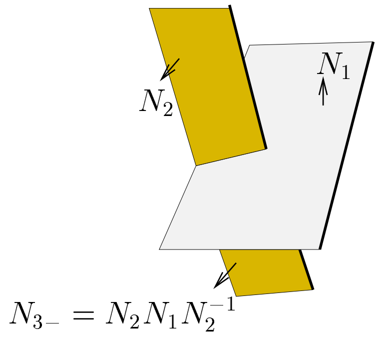

Figure 4: A typical intersection.

$$N_{3-} = \begin{pmatrix} 0 & -1 & 1 & -2 \\ -1 & 0 & 4 & 1 \\ 0 & 0 & 0 & -1 \\ 0 & 0 & -1 & 0 \end{pmatrix}.$$

The classical monodromy group generated by any two of these linear maps has a $\mathbb{Z}_3$ symmetry upon cyclically permuting the indices 1, 2 and 3−. The relations are

$$N_{3-} = N_1^{-1} N_2 N_1 = N_2 N_1 N_2^{-1} \quad \text{and cyc. perms}$$

One of these can be seen in figure 4, a close-up of an intersection in figure 3. The relation above also justifies the imposition of a common meeting point for the cuts — all small closed loops in the vicinity of the origin have trivial monodromy.

The classical mondromy associated with each root acts on states with the same subscript by shifting them two places higher up their respective tower. It moves states in the other towers to different towers, sometimes to a tower we have met already, and sometimes to more exotic ones, which we shall encounter later.

$$\begin{aligned} Q_i^n N_i &= Q_i^{n-2} \\ Q_1^{n+2} N_2 &= Q_{3+}^n = Q_2^n N_1^{-1}, \\ Q_2^n N_1 &= Q_{3-}^n = Q_1^n N_2^{-1}. \end{aligned} \qquad (2.1)$$

It still remains to place the curve of marginal stability described in [7]. If, as in figure 6, we take 2-dimensional sections of our space by considering a vertical half-plane projecting radially outwards from $u = 0$, then the trefoil will intersect it in two points. We claim the CMS, defined as the set for which $\mathrm{Im}[\alpha_1.a/\alpha_2.a] = 0$, lies between them, and for our purposes it will be sufficient to represent it as a straight line between them. This line will rotate as one rotates the 2-dimensional radial section about the $u = 0$ axis, forming a twisted ribbon with the trefoil as its boundary.

JHEP08(2001)031

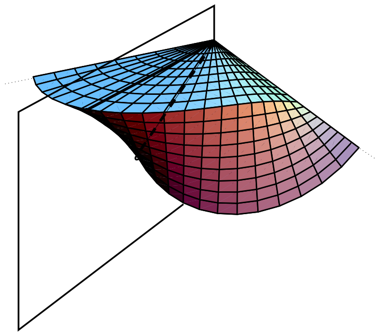

Figure 6: Radial sections of curves aid exposition.

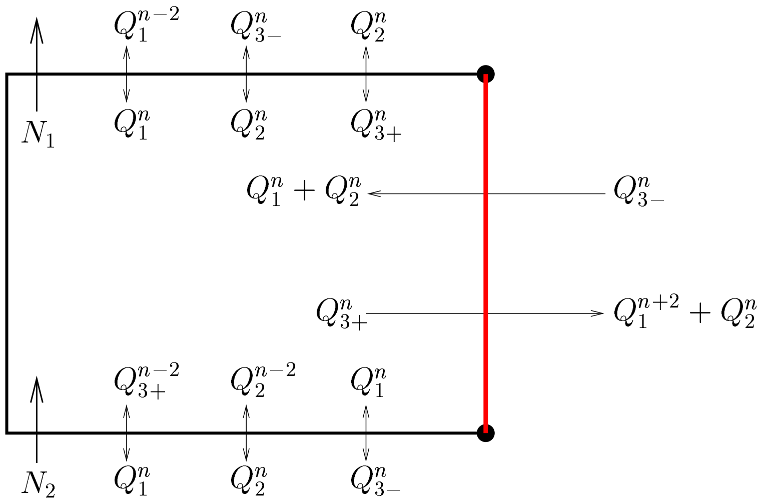

Figure 7: The classical BPS spectra in the 3+ and 3− domains.

From now on, we shall concentrate on the third of the space for which N_1 is the monodromy on top (with N_2 on the bottom) and call this the 1,2 sector. Sometimes we choose to show the branch cuts bent away from being straight to make space to describe all the states present between them. figure 7 shows how the branch cuts and the CMS conspire to partition the 1,2 sector into two domains, one connected to the weak-coupling limit at $u = 0$ with Q_{3+}'s, not Q_{3-}'s in the BPS spectrum, the other to the one at $u = \infty$ with Q_{3-}'s, not Q_{3+}'s.

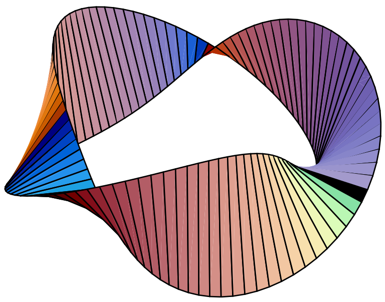

Figure 5: The classical CMS.

As the Casimir variables are invariant under the action of the Weyl group, we have no right to expect that always the α_3 tower is deformed as opposed to the other two. Putting α_1, α_2 and $-\alpha_3$ on the same footing, we allow for weak-coupling regions where any two of these roots are regarded as simple, while the tower corresponding to the third one has shifted electric charges.

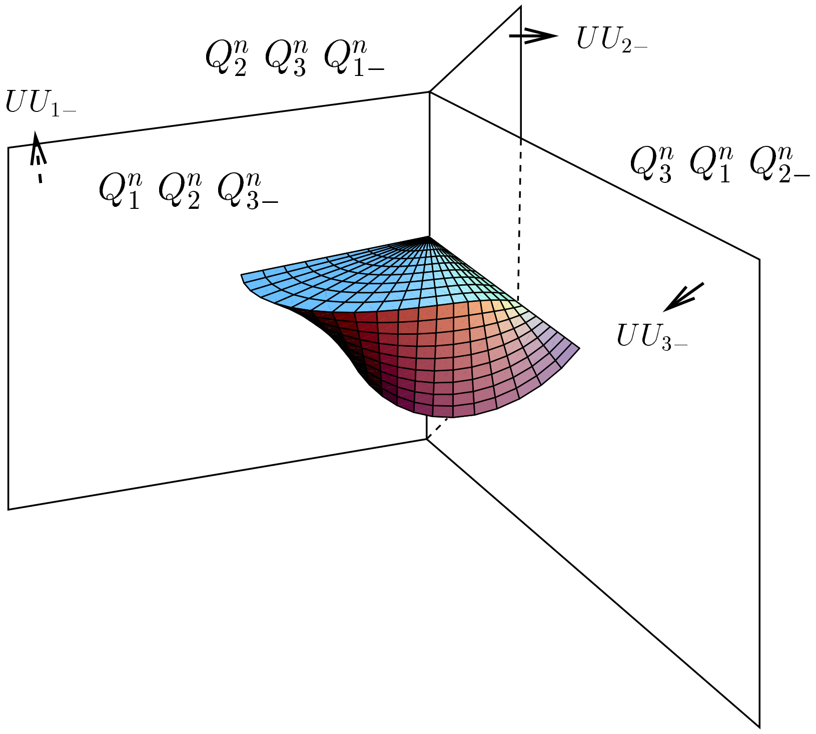

Figure 8: The U's rotate which of the towers of BPS states has shifted electric charge. Only one third of the curves is shown.

Therefore the space must be partitioned such as to have six disjoint weakly-coupled regions containing towers of BPS states $\{1,2,3-\}$, $\{1,2,3+\}$, $\{1,2-,3\}$, $\{1,2+,3\}$, $\{1-,2,3\}$ and $\{1+,2,3\}$. This can be performed by the addition of three branch cuts seen as vertical half-planes from $u=0$ to $u=\infty$, at angles such that they project along the lines of intersection of the previously described classical branch cut. The monodromies at these cuts are given by UU_{i-} which are described by the following matrices in our basis, with directions as indicated in figure 8, where only the cuts and curves in the 1,2 sector are drawn.

$$U=\begin{pmatrix}0&1&0&0\\-1&-1&0&0\\0&0&-1&1\\0&0&-1&0\end{pmatrix},\qquad U_{1-}=\begin{pmatrix}-1&-1&-2&-1\\1&0&1&1\\0&0&0&-1\\0&0&1&-1\end{pmatrix}.$$
$$U_{2-}=\begin{pmatrix}-1&-1&1&1\\1&0&1&-2\\0&0&0&-1\\0&0&1&-1\end{pmatrix},\qquad U_{3-}=\begin{pmatrix}-1&-1&1&-2\\1&0&-2&1\\0&0&0&-1\\0&0&1&-1\end{pmatrix}.$$

The charges of the states not yet defined (e.g. Q_{2+}^n, Q_3^n), can be obtained by cyclically permuting α_1, α_2 and $-\alpha_3$ from the analogous state previously listed. Note U_{3-} cyclically permutes Q_1^n, Q_2^n and Q_{3-}^n, the BPS spectrum in the outer domain of the 1,2 sector. Similarly for the other U_{i-}. There also exist U_{i+}'s permuting the towers of the inner spectra. U permutes the subscripts 1, 2, and 3, acting as an exact $\mathbb{Z}_3$ on the moduli space, rotating it about $u = 0$ by $2\pi/3$.

3. Higher spin multiplets

Now let us consider the case for non-aligned Higgs fields. In [12] it is claimed that the two BPS spectra for the 1,2 sector should contain BPS states in higher spin multiplets. The analysis, based on the Scherk-Schwarz mechanism, results in the prediction of states with charges $(\alpha_3, n\alpha_3 - s\alpha_1)$ for the outer domain, and $(\alpha_3, n\alpha_3 + s\alpha_1)$ for the inner domain, with $s \in \mathbb{Z}^+$ being twice the spin of the highest state in the multiplet. Passing the new outer states up through the classical branch cut, they are acted upon by the monodromy N_2N_1, giving states with charges $(\alpha_1, (n-1)\alpha_1 + (s-1)\alpha_2)$. Repeating the circuit gives $(\alpha_2, n\alpha_2 + (s-1)\alpha_3)$, and a third repetition sees us return to the original higher spin towers. Therefore we predict the existence of these new towers of states at weak coupling. Similarly for the inner domain with the sign of s reversed, and for the 2,3 and 3,1 sectors, with α_1, α_2 and $-\alpha_3$ cyclically permuted. Any branch cut or CMS which might posssibly alter the spectrum during the course of this triple circuit as a means of circumventing this existence argument would necessarily touch either $u = 0$ or $u = \infty$ and so could only further partition the set of states at weak coupling, not eliminate the space carrying the unwanted spectrum completely.

It turns out that none of these higher spin states exist at strong coupling. They all decay on a series of CMS's labelled D's and F's which circle around both arms (as viewed in the 2D section). We are therefore at liberty to consider both the quantum and classical pictures without the higher multiplets interfering. We shall return to describe the necessary CMS's soon, after we have motivated the introduction of further notation.

4. Non-perturbative effects for weak and moderate coupling

We now include the effect of instantons in this picture. For all SU(N) these cause a bifurcation of the singular surface, seen as an effective shift in the top Casimir (v for SU(3)) proportional to $\pm\Lambda^N$. For SU(2), a *quantum* branch cut appears between the two singular points, and so one may trace paths braiding around the two singularities. For SU(3), it is similarly the case that the two trefoils we now have will possess a quantum branch cut between them. As Re[v] is the vertical direction in the 3-dimensional sections we take, the trefoils are nothing but two copies of the same trefoil vertically translated by an amount proportional to Λ^3. The quantum branch cut is therefore a ribbon (with no twists) composed of vertical lines between the two trefoils. (see figure 9).

The three classical monodromies split into six quantum ones, as detailed in [10]. To each classical monodromy N_i we associate a pair of quantum monodromies M_{2i} and M_{2i-1}, with $M_{2i}M_{2i-1} = N_i$. As for SU(2), the M's must be parabolic, meaning their repeated action on a state adds a constant amount each time to the charges of that state, forming a tower isomorphic to $\mathbb{Z}$. Thus we find for SU(3), acting in four real dimensions, that they each preserve a 2-dimensional subspace, acting as a shear on the whole charge space by a vector in the invariant subspace. Each M is therefore specified uniquely (modulo direction) by a charge vector (g, q). By the mass formula, a BPS state with charge (g, q) will become massless at a fixed point of this monodromy, i.e. at a singularity where the corresponding branch cut ends.

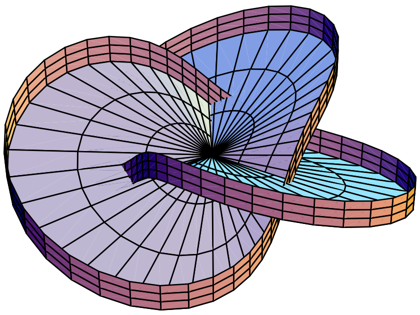

Figure 9: The classical and quantum branch cuts for large R.

The matrix corrresponding to charge (g, q) is given by

$$M_{(g,q)} = \left(\begin{array}{c|c} 1 + q \otimes g & q \otimes q \\ \hline -g \otimes g & 1 - g \otimes q \end{array} \right).$$

We have some freedom to label charges, and we do so as to put ourselves on a sheet where states have simple quantum numbers. Following [10] we choose $M_2 = M_{(1,0,0,0)}$, and $M_3 = M_{(0,1,0,0)}$. The odd M's, and similarly the even M's obey the same relation as the N's:

$$\begin{aligned} M_6 &= M_2^{-1} M_4 M_2 = M_4 M_2 M_4^{-1} \\ M_5 &= M_1^{-1} M_3 M_1 = M_3 M_1 M_3^{-1} \text{and cyc.} \end{aligned} \tag{4.1}$$

Due to the cyclic symmetry, because M_2 and M_3 commute (the charge vectors lie in each other's invariant subspace), M_4 and M_5 commute, as well as M_6 and M_1. If we associate the even M's with the cut continuing from their respective N, (M_{2i} with N_i), pointing inwards toward the origin as in figure 10, we can then find which states become massless at which places. We always get the same pattern: For the arm with label $i\star$ (where $\star$ is blank, $+$ or $-$), the state becoming massless at the top singularity is $Q^1_{i\star}$, and at the other is $Q^0_{i\star}$ from above and $Q^2_{i\star}$ from below.

Thus, at this level, it seems each arm is just a little SU(2) microcosm, nothing more than an area where the SU(3) solution is dominated by an embedded SU(2) associated to one of the root directions. We shall continue the pursuit of this idea later.

In this region of moduli space we shall encounter two types of curves of marginal stability, the L's and the G's (for local and global). Further out, encircling both arms and never coming close to them are a collection of curves labelled D's and F's

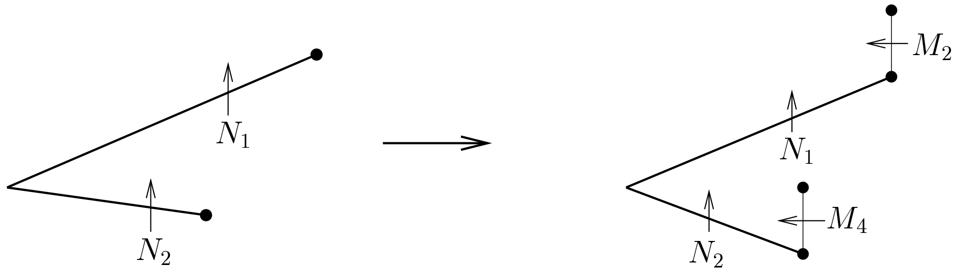

Figure 10: Our choice of cuts.

upon which all the higher spin states decay to the simpler spectrum given in [7]. We start with the premise that no CMS has a boundary, and that occasionally they may touch the singular surface. It is from this that we glean information about them. At any particular point on a CMS, a decay may take place involving one state decaying into two others with charges that sum to the original. The curve does not see these states in particular, but the whole lattice of charges generated by integer linear combinations of any two of them. Any possible decay involving three states with charges on the lattice which sum to zero may happen at some point along the curve, indeed many at once. Most will not occur, either as none of the states is present, or for kinematic reasons, or for some other reason that a decay into an exotic particle is excluded. Sometimes, also, a decay occurs which has no effect on the spectrum as parent and daughter states are present on both sides of the curve anyway. If a curve has no effect on our spectrum at all, we say it is *irrelevant*. If a decay takes place at one point of a curve, it will also occur in the vicinity of that point. It will continue along the curve, including through branch cuts (whereupon each state is individually acted upon by the monodromy) unless it reaches a point where the curve adjoins a singularity, whereupon the light particle 'swaps sides', as which of the other two states is most massive changes, and the arrow of the decay process reverses. Arrow reversal is a necessary condition for the curve to touch a singularity. Later we shall meet accumulation points, which are the next best thing to singular points, and the curves behave characteristically there too.

We presume that if a curve passing by a singularity has upon it a decay involving the state which becomes massless at that singularity, then the curve will touch the singularity. As we rotate our 2-dimensional radial section, any CMS (now a line) touching one of the four singularities will do so regardless of the position of the singularity (the top and bottom arms, each with their singularity pair, will rotate around each other). Even when the singularity passes through a branch cut the curve can follow it, and the states involved in the decay will be the original ones acted upon by the monodromy (which is linear). We say that the curve is *generically adjoined* to the singularity.

Figure 11 shows the effect of generic adjoinment on a CMS. Whatever the curve does locally around each singularity pair, if it touches one singularity from each arm

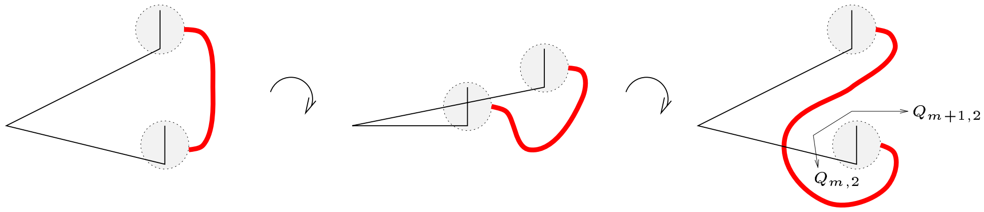

Figure 11: The CMS becomes twisted as we rotate the radial section. This allows some states to wrap around before decaying. In the shaded circles the CMS has fixed but undetermined topology.

then globally it will become twisted. There will exist, superposed, a curve with more twists and with the same type of decay but with all three states raised to a higher position on their tower (actually for one twist $n \mapsto n+2$). If we define states

$$Q^n_{m,1} = Q^n_{3-} N^m_1\,, \qquad Q^n_{m,2} = Q^n_1 N^m_2\,,$$

then one can also see from the diagram that states of high $|m|$ will exist close to the singularity pairs. The charges of these states and analogous ones are:

$$\begin{aligned}
Q^n_{2m,1} &= (\alpha_3, -(2m+1)\alpha_1 + n\alpha_3)\,,\\
Q^n_{2m-1,1} &= (\alpha_2, 2m\alpha_1 + n\alpha_2)\,,\\
Q^n_{2m,2} &= (\alpha_1, (n-1)\alpha_1 + 2m\alpha_3)\,,\\
Q^n_{2m-1,2} &= (\alpha_3, -\alpha_1 + n\alpha_3 - 2m\alpha_2)\,,\\
Q^n_{2m,3-} &= (\alpha_2, -(2m)\alpha_3 + n\alpha_2)\,,\\
Q^n_{2m-1,3-} &= (\alpha_1, -2m\alpha_3 + (n-1)\alpha_1)\,.
\end{aligned} \tag{4.2}$$

We have overdefined the states by a factor of two. The $Q_{m,i}$ need only even m to describe them. The odd ones are equivalent under the relation

$$Q^n_{2m,i} = Q^{n-2m}_{-(2m+1),i+1}\,, \qquad i \in \{1,2,3-\}\,.$$

Note that $Q^n_{3-} = Q^n_{0,1} = Q^n_{-1,2}$ and $Q^n_{3+} = Q^n_{-2,1} = Q^{n+2}_{1,2}$.

These $Q^n_{2m,i}$ have the same (g,q)-charges as the multiplets of higher spin (specifically, as spin multiplets with maximal spin 3/2, 5/2, 7/2, ...) as defined in [12] which we know to exist at weak coupling. Of course we doubt that they also possess similar higher Lorentz quantum numbers — i.e. that passing through a branch cut can notch up or down a states' spin — but other strange things can happen. The analysis depends only on the (g,q) charge of the state, so even (as we believe) if they are not the same, these states will behave identically for our purposes.

The other half of the general spin states present at the weak-coupling boundary, those with integer spin, we call R's.

$$R^n_{2m,1} = (\alpha_3, -(2m)\alpha_1 + n\alpha_3)\,,$$

$$
\begin{aligned}
R^n_{2m-1,1} &= (\alpha_2, (2m-1)\alpha_1 + n\alpha_2)\,, \\
R^n_{2m,2} &= (\alpha_1, (n-1)\alpha_1 + (2m-1)\alpha_2)\,, \\
R^n_{2m-1,2} &= (\alpha_3, -\alpha_1 + n\alpha_3 - (2m-1)\alpha_2)\,, \\
R^n_{2m,3-} &= (\alpha_2, -(2m-1)\alpha_3 + n\alpha_2)\,, \\
R^n_{2m-1,3-} &= (\alpha_1, -(2m-1)\alpha_3 + (n-1)\alpha_1)\,.
\end{aligned} \tag{4.3}
$$

These transform amongst themselves under the classical monodromy group (let alone under the subgroup of this we get when we include CMS's). They do not include any states which become massless, limiting our ability to describe the CMS's upon which they decay.

We now have the labels to state succinctly the BPS spectrum at both weak coupling points:

$$
\text{At } \left\{ \begin{matrix} u = \infty \\ u = 0 \end{matrix} \right\} \text{ we have } Q^n_{2m,i} \ \forall i \in \{1, 2, 3-\}, m, n \in \mathbb{Z}\,, \left\{ \begin{matrix} m \geq 0 \\ m < 0 \end{matrix} \right\}.
$$

$$
\text{At } \left\{ \begin{matrix} u = \infty \\ u = 0 \end{matrix} \right\} \text{ we have } R^n_{2m,i} \ \forall i \in \{1, 2, 3-\}, m, n \in \mathbb{Z}, \left\{ \begin{matrix} m > 0 \\ m < 0 \end{matrix} \right\}.
$$

There are a number of possible types of decay curves, ones involving three Q's (G's (and also L's)), involving QQR (the F's), QRR (the E's) and RRR (the D's).

In regions of weak coupling the higher spin multiplets have larger charges and are hence more massive. We would therefore expect them to decay into smaller, lighter multiplets. Indeed, the sum of the (maximal) spins of decay product states would be equal to the (maximal) spin of the original one. This implies neither of the product states are of higher spin than the original. The decay of a multiplet with highest spin m can thus happen in a variety of ways according to the various partitions of m. The way we believe it to happen is that the spin decreases one-half-at-a-time on a series of curves F where the heavy multiplet necessarily alternates between having integer or half-integer maximal spin as it cascades down, $Q \to R \to Q \to R \ldots$, while giving off a $Q_{0,i}$ each time, and terminating also in a $Q_{0,i}$. We also allow for this queue to be jumped by R's decaying into two lower R's, the sum of whose spins equal the original. We do not believe the Q's jump the queue into lower Q's or lower R's, but it would make little difference if it turned out to be the case.

The uncomplicated shape of a typical curve F is shown in figure 12 — it justs wraps infinitely many times around the tori on which the trefoils lie. Each F is associated with a particular spin. Although the labels change slightly while the curve is in-between the classical branch cuts, the spin remains the same. On the outer region, passing either a $Q^n_{2m,i}$ or an $R^n_{2m,i}$ up through both classical branch cuts takes $i \mapsto i+1$ and $n \mapsto n-2$. After three cycles one returns to the same tower $(2m, i)$ but $n \mapsto n-6$. A similar thing happens if one starts from the inner region, but the notation is not so transparent. Now the towers labelled by subscripts

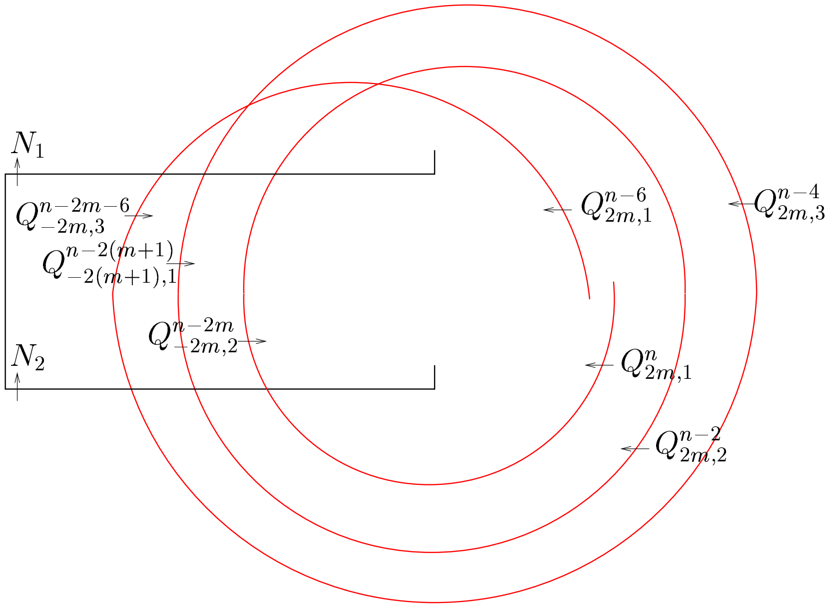

Figure 12: A typical curve F.

$(2m-2,1)$ have the same spin as $(2m,2)$ and $(2m,3)$ (as states of the same spin are now related by U_{3+} instead of U_{3-}) and these three towers rotate into each other as expected. We therefore need only consider the decay for one label i as the cases for the other two i will be generated by following the curve around one cycle in either direction (of course the decay products also have their $\mathbb{Z}_3$ label i incremented or decremented). To cover all n in each tower, we shall need six copies of each curve, one for each n mod 6. We shall also need two types of curve, one for a Q to an R with one half less maximal spin (plus a low Q), and one for an R to a Q with one half less spin (plus a low Q). There turn out to be two equally valid curves of each type:

$$Q^n_{2m,1} \longrightarrow R^{n-2m}_{2m,2} + Q^{n-2m+1}_{0,3}$$
$$Q^n_{2m,1} \longrightarrow R^{n+2m-1}_{2m,3} + Q^{n-1}_{0,2}$$

and

$$R^n_{2m,1} \longrightarrow Q^{n-2m+1}_{2(m-1),2} + Q^{n-2(m-1)}_{0,3}$$
$$R^n_{2m,1} \longrightarrow Q^{n+2(m-1)}_{2(m-1),3} + Q^{n-1}_{0,2}$$

The D curves which allow multiplets with integer maximal spin m to 'jump the queue' also have the same simple shape as the F's. There is one for each bipartition of m, namely for some $m = k + l$

$$R^n_{2m,1} \longrightarrow R^{n-2k}_{2k,2} + R^{n+4k}_{2l,3}\,.$$

We may now forget about the higher spin multiplets and the D's and F's and return our focus to the CMS's at stronger coupling.

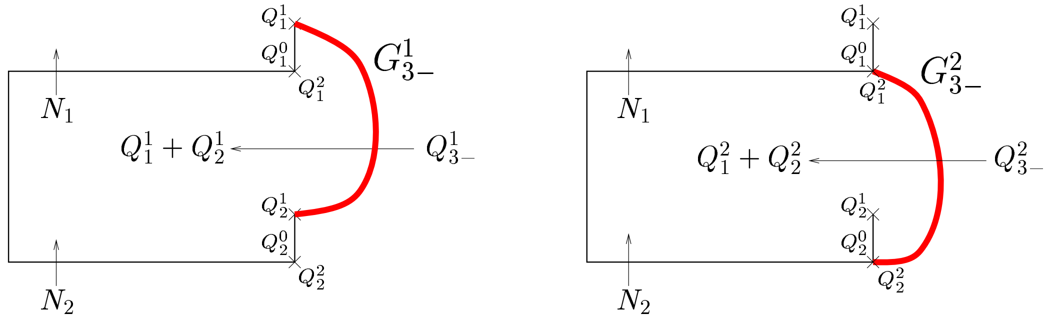

Figure 13: CMS's which will generate all the G's. The states becoming massless at each singularity are labelled.

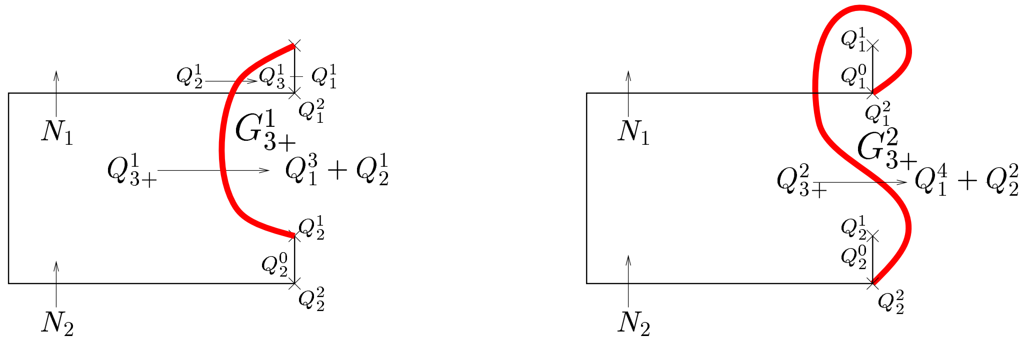

Figure 14: Rotation of figure 13.

5. The global curves

We are now in a position to inspect how the classical CMS splits as we include non-perturbative quantum corrections. An infinite number of decays occur on the classical CMS, ones for all $Q^n_{3\pm}$. We find the curve does not just bifurcate, but that each piece also 'unravels'. We begin by looking at two test segments, and find that under twisting they generate the whole of the G's.

It could be said that the role of the classical CMS was to partition each of the sectors into two domains. This must remain the job of the G's, which coalesce to form the single CMS as we turn off the non-perturbative effects. With this in mind, let us begin with two curves whose presence is staring us in the face, namely the decay of Q^1_{3-} into $Q^1_1 + Q^1_2$, which will touch the top singularity of each arm in the 1,2 sector, and $Q^2_{3-} \to Q^2_1 + Q^2_2$ which will touch the bottom of each pair. These are displayed in figure 13.

As we rotate the 2-dimensional section the curve twists. U-covariance demands that if after a half twist in the positive sense (such that the other arm is now on top and we are in the 3,1 section), we superimpose this curve back on the original section whilst multiplying by UU_{3-} (i.e. cyclically permuting back the indices), then this curve must also exist. We find it to be figure 14.

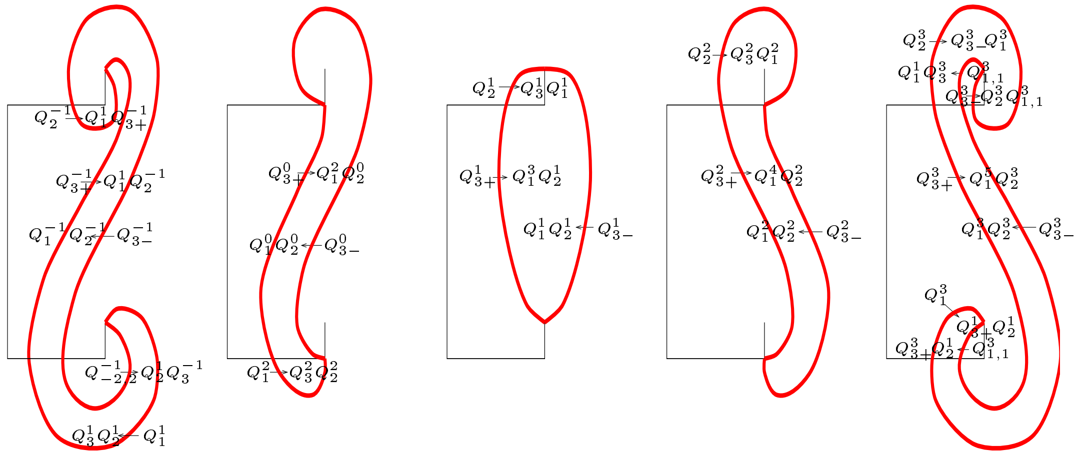

Figure 15: More G_{3-} and G_{3+}'s. The pattern continues to the left and right.

Repeated twists of the arms around each other in this manner suffices to generate from just the two curve segments in figure 13 all the curves (or rather all parts of the same two curves) necessary to partition the region into two domains each carrying one of the towers 3− or 3+. A few of these are shown in figure 15.

6. The cores

In the 2D-sections we have drawn, each arm looks remarkably like a copy of the SU(2) moduli space. It has two singularities, a quantum branch cut between them, and a classical one tending off to infinity. SU(3) has three natural SU(2) embeddings, one for each root. As each of our arms are also associated with one of the three roots, it is natural to identify the region near the two singularities of an arm as the place where the SU(3) coupling is strong only in the projection onto the relevant SU(2) subspace. To complete this picture we also need the CMS corresponding to the unique decay curve in the pure SU(2) case. For the arm labelled by i, which is associated to the α_i direction and has classical and quantum monodromies N_i and M_{2i} respectively, we find a CMS which is topologically a circle passing through both of the singularity pair. On the left of the quantum branch cut all the states Q_i^n decay to a combination of Q_i^0 and Q_i^1. On the right of the cut they decay to Q_i^1 and Q_i^2. This is shown in figure 16. We call this CMS L_i. Returning to the whole picture of the trefoil pair, we see that the L_i form one continuous closed tube L in the shape of a trefoil, lined on the top and bottom by the two trefoils that are the two singularities, as seen in figure 17.

If we concentrate on the α_1 arm, we notice that the Q_2 and Q_3 towers are not blocked from M_2 by L_1, nor are the $Q_{m,1}$ which are these states after being wrapped around the α_1 singularity pair a number of times. Luckily the G's fulfill an unexpected dual role, limiting the states getting inside L to exactly those which

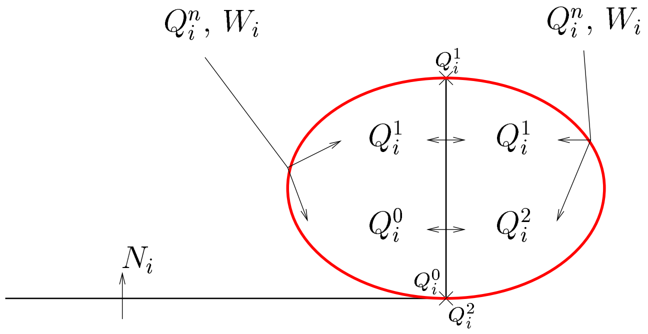

Figure 16: The region where the α_i direction is strongly coupled.

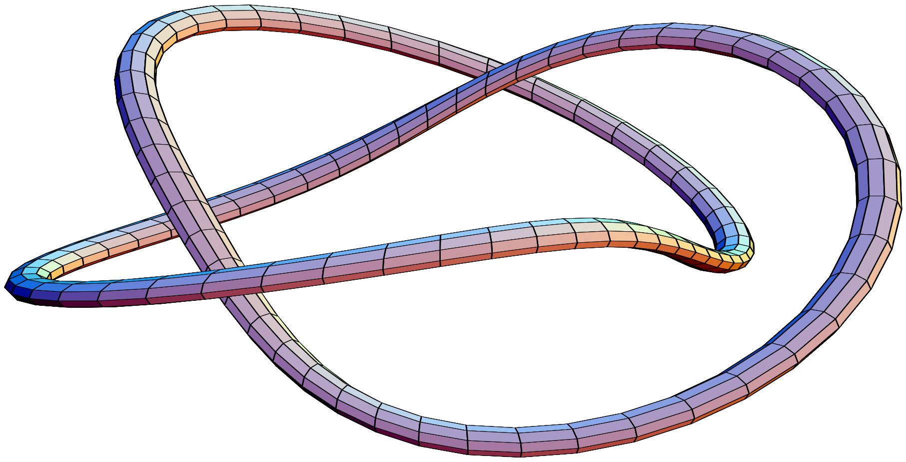

Figure 17: The CMS L which bounds the core.

transform nicely through the quantum branch cut there. From now on we shall refer to this region inside L as the *core*.

After the decay of the higher spin multiplets we are left with three towers at each point, Q_1, Q_2, and Q_{3+} or Q_{3-}. If we are considering the core associated to the α_1 arm, we think of these towers as Q_1, $Q_{-1,1}$, $Q_{-2,1}$ and $Q_{0,1}$; and for that with the α_2 arm, $Q_{0,2}$, Q_2, $Q_{1,2}$ and $Q_{-1,2}$ respectively. When a curve twists a lot of times around a core, one finds another cascade of decays. Here what happens is that the n index, which distinguishes states within a tower, is preserved, but m increases (or decreases if the curve wraps in the other sense) until it has reached the lightest state it can with that value of n. This occurs for

$$n = 2m + 1\,, \qquad n = 2m + 2\,, \qquad n = 2m + 3\,.$$

We label these states $S^{-1}_{m,i}$, $S^{0}_{m,i}$ and $S^{1}_{m,i}$ respectively. For all the intermediate states in the cascade, we find they are confined to a strip bounded both away from the core and from the weak coupling regions, and by the classical branch cut in a way shown in figures 18 and 19. The other decay products are all Q_1's which we know to be excluded from the core by L_1. The special states $S_{m,i}$ are confined merely to strips

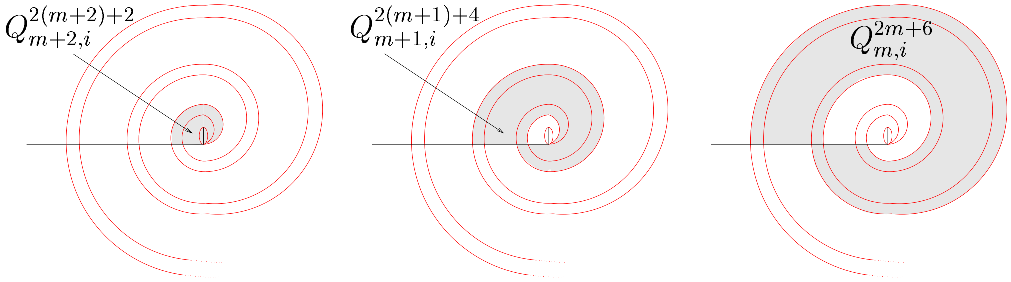

Figure 18: A sketch of the existence domains of some states around a core.

which end at the core. $S^0_{m,i}$ is invariant through the quantum monodromy in the core, and the other two sets map into each other by the action of the monodromy, the $S^{-1}_{m,i}$ on the left and $S^1_{m,i}$ on the right.

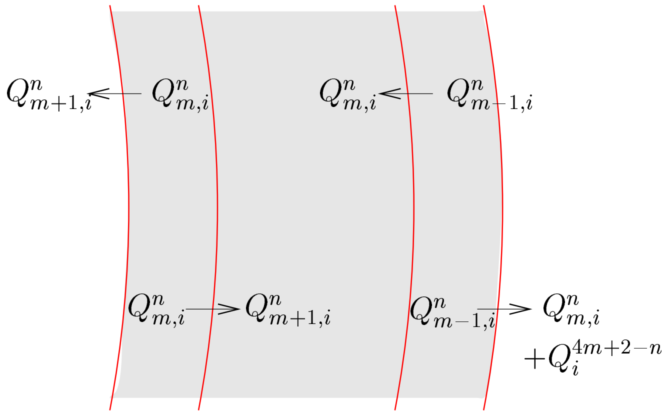

Figure 19: The decays involved in an existence domain strip.

We now see that we have 3 towers of states within each core L_i (though only two at any point), the $S^{-1}_{m,i}$, $S^0_{m,i}$ and $S^1_{m,i}$. This time the label is on the bottom, and we see that in a sense n and m have swapped roles. These are strong coupling towers, where the separation of charge is not that of a gauge boson, but of the difference between two of these. For each i, one might expect a BPS state to exist with such charge, which we believe to be the case, and later we explain their necessity within the model. We expect that such a tower can be seen to be formed from a dual model, weakly coupled at this core, with the charge angle in the monopole moduli space translating back to lie in a different direction within SU(3).

7. The meeting of the cores

Even for the classical case, the trefoil degenerates at a certain S^3 radius $R = \sqrt{3}\Lambda$, its innermost parts pinching together while the knot 'unties', and after which three unlinked circles remain. As we decrease the S^3 radius in the full quantum theory,

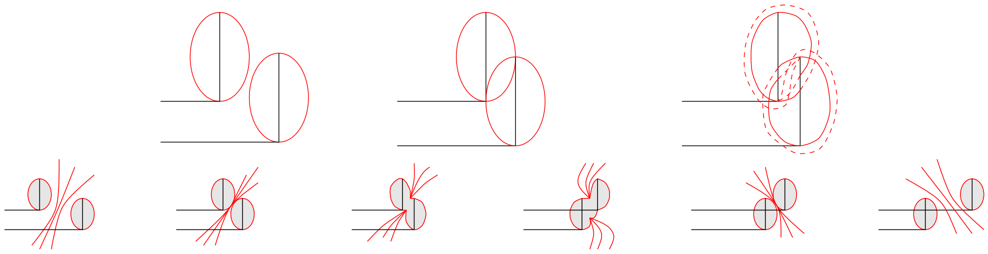

Figure 20: Two possible scenarios for when two roots become strongly coupled.

the distance between the two trefoils increases, as does the core between them. At a critical radius something gives — the trefoils pass through each other at three points. Also, at this same radius, both trefoils degenerate at their centre. Further decreasing the radius, the intersection with the singular surface takes the form of six circles, two for each root, still with a core between them.

One can check that the top singularity of the pair associated to the bottom arm may pass with impunity through the quantum cut of the top arm, between its singularity pair. This is what happens for R only a little below the critial value. The cores in this case must wrap and tangle, or merge, as seen in figure 20. That they merge is by far the most elegant idea. We have been unable to find consistent models incorporating wrap and tangle and believe them to have generic problems. We thus consider the picture presented in the bottom half of figure 20. One can see that the set of G curves wrapped around each core are necessarily squeezed to a point, then bisected. We call a point through which an infinite number of CMS's pass an *accumulation point*.

8. Accumulation points

We remarked before that a CMS depends on the lattice generated by integer linear combinations of any two of the three states involved in a decay across it. Conversely, any two charges give a potentially relevant CMS. We label the equivalence classes of CMS's, or two-generator lattices as $[(g_1, q_1), (g_2, q_2)]$.

In this notation $L_i = [(0, \alpha_i), (\alpha_i, 0)]$, for instance. Other curves of subsequent importance are

$$\beta = [(0, \alpha_i), (0, \alpha_j)]\,, \qquad \gamma_{ij}(n, n') = [Q_i^n, Q_j^{n'}]\,.$$

We label

$$\gamma_{ij} = \bigcap_{n,n'} \gamma_{ij}(n, n')\,.$$

Although we can say little about where two curves cross, if they do cross then the combined constraints may imply that other curves also pass through this point too.

JHEP08(2001)031

From figure 20 we can see that there must be points where L_1 crosses L_2. It would be helpful if all the wrapped G's could then be shown to accumulate here too. $L_1 \cap L_2$ is not sufficient, but $L_1 \cap L_2 \cap \beta$ is equivalent to $L_1 \cap L_2 \cap \gamma_{12}$ which is very strong indeed.

If the cores merge then it might seem that L_1 and L_2 have a boundary on the accumulation points where they meet. This cannot be the case, so we must assume that we have so far overlooked components of these curves encircling the 'wrong' cores. All these curves act within a tower, mapping elements of the tower into the two with the lowest value of n. Towers are labelled by subscripts m and i. As L_1 encircles the α_1 core it falls back on itself to form a closed curve as in the SU(2) case. Wrapping once, we find the relation $L_3 = L_2 N_1$, and continued wrapping will create a different curve with each rotation. Those with an even number of cycles from L_3 behave differently to those with an even number of cycles from L_2. In the former case

$$\forall n\,, \quad Q^{n-2m}_{(2m+1),1} \longrightarrow Q^{1}_{-(2m+1),1} + Q^{0}_{-(2m+1),1} \Leftrightarrow \forall n\,, \quad [W_2, Q^{n-2m}_{-(2m+1),1}]$$

If, as is likely, any two of these meet, then they all meet, at $[\beta \cap L_2]$. Similarly for an odd number of cycles (those associated with the tower $Q_{2m+1,1}$), they all meet at $[\beta \cap L_3]$. Odds cross evens at different points in all cases. Finally, just as L_2 is a special case of one of the family wrapping around the α_1 core, associated to the $Q_{2m,1}$'s, then L_1 is a special case of a family around the α_2 core, associated to the $Q_{2m,2}$'s, which must also be boundaryless when the cores merge. Therefore we must consider L_1 to be a special case of this family, which acts slightly differently around the α_1 core. Here we find that a rotating around once maps $(2m, 2) \mapsto (-2m, 2)$, and so performing two cycles maps one back to the same tower. We might still expect an accumulation point where L_1 (associated to $Q_{0,2}$) would intersect the curves associated to all the other $Q_{2m,2}$'s, which would happen when $\beta \cap L_1$. Maybe this does not occur until the cores merge, however. The addition of all these curves also shields the core L_i from the other two gauge bosons W_j and W_k.

When the cores first touch, we envisage that all six accumulation points coalesce as in figure 22. Thus we have $(\beta \cap L_1) \cap (\beta \cap L_2) \cap (\beta \cap L_3)$. This then guarantees that all the wrapped G's (and more besides!) will accumulate at this point. After this, the six points separate into two sets of three, each with the same conditions. While the cores pass through each other, these accumulation points rotate around the merged core until, at the point where the cores separate again, the two points have swapped position, top-for-bottom and bottom-for-top.

9. Double cores

The merging of cores presents us with new problems to resolve. Clearly, without the addition of more curves, we find ourselves with the union, not the intersection

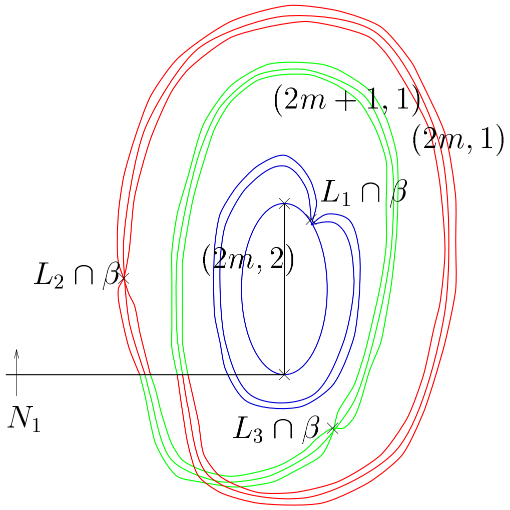

Figure 21: The curves encircling the α_1 core.

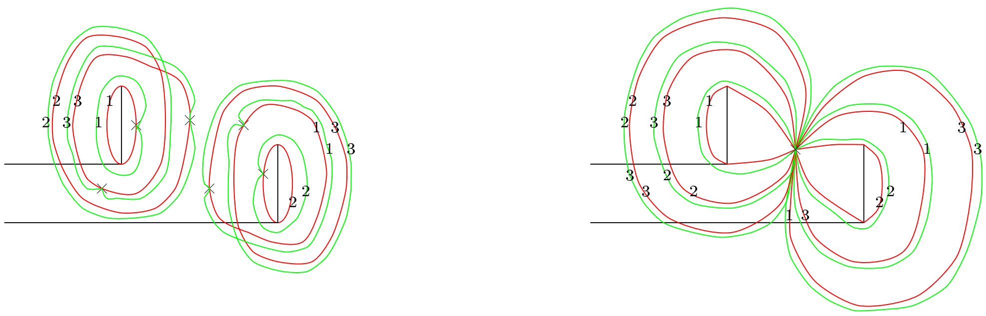

Figure 22: The accumulation points merge as the cores touch.

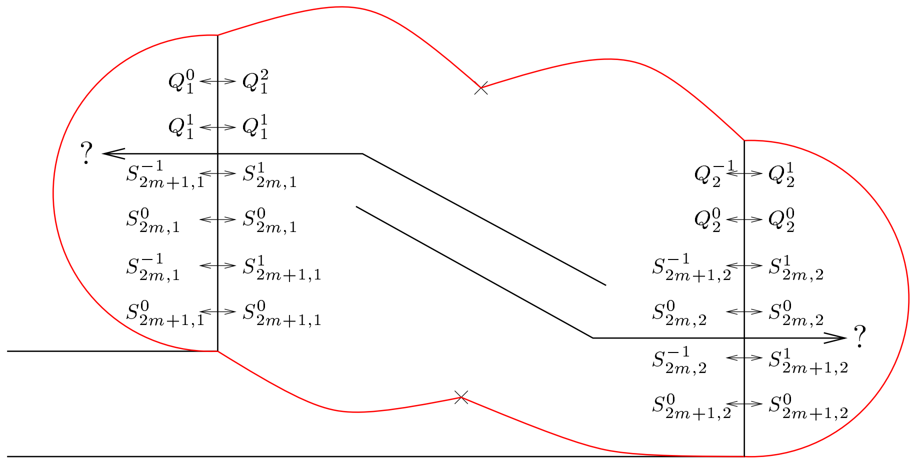

Figure 23: The states native to each core are alien to the other one.

of the spectra within the cores L_i and L_j. More worryingly, the strong coupling towers of states $S_{m,i}$ and $S_{m,j}$ do not transform well through the opposite quantum monodromies, as seen in fig. (23).

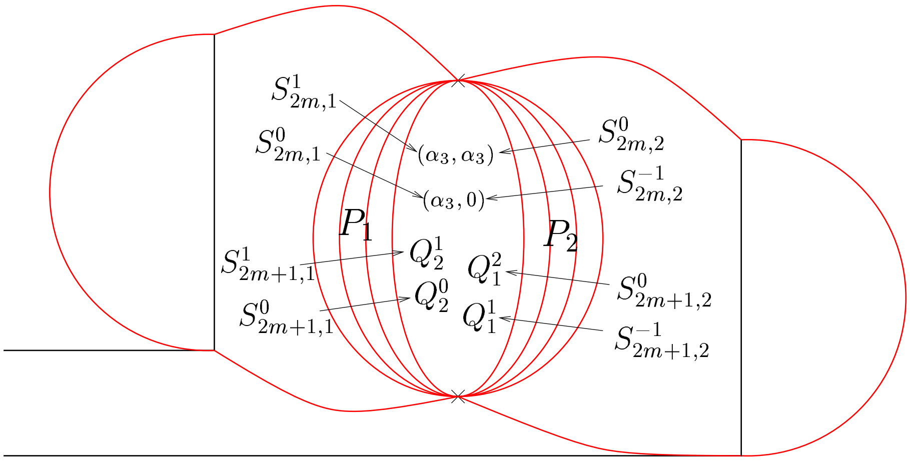

Figure 24: There is a double core region from which the S's are excluded, but four new states are created.

What is more likely is that families of curves form between the accumulation points upon which nearly all the states of both cores decay, to leave a region in the centre with just a few (indeed a finite number) of states which transform nicely through both quantum mondromies. We call this central region a *double core*. The new curves are necessarily circular in our 2D-sections, hence spherical in 3-dimensions and 3-spherical in the full 4 dimensions. Thus we find three bounded regions for which two root directions are strongly coupled, and within each of which lies a double core carrying a finite number of BPS states.

From figure 24 one can see that there are eight families of curves required to fulfill this task. In each case one is met with a cascade of $(m, i) \mapsto (m-2, i)$ giving as a by-product $2P_i$. If we define the massive gauge bosons W_1, W_2 and W_3 as having charges $(0, \alpha_1)$, $(0, \alpha_2)$ and $(0, -\alpha_3)$ respectively, then P_i has charge equal to the difference $W_{i-1} - W_{i+1}$. Thus the P_i seem in some way to perform the role of gauge bosons within the core. P_i is invariant under the monodromies of the α_i arm. Under the other classical monodromies it transforms into the other two P's, but under the other quantum monodromies it is not so well behaved — the states into which it transforms do not have unit magnetic charge. These rogue states decay on a set of curves, for each rogue state one curve emanating from the top, and one from the bottom of the cut across which the rogue state is created. As all these curves must pass through the accumulation points, they must touch, and hence bound the existence domain of the rogue state. The decays on the curves are back to a P plus the state becoming massless at the singularity through which the curve passes.

The P_i do not exist at weak coupling, and most likely decay to gauge bosons on a curve similar to the D's and F's but this time closed after three cycles, most probably as $P_i \to 2W_{i-1} - W_i$. Within this curve all three P_i exist at every point. Recall that all the gauge bosons are shielded from the core by the L_i.

Figure 25: $R^0_{0,1}$ and $R^1_{0,1}$ are confined to 3-spheres around the double core.

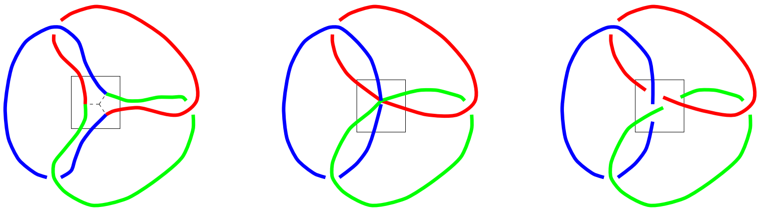

Figure 26: The A_2 singularities highlighted from the point of view of the bottom of the quantum cuts.

Finally, note that $R^0_{0,1} = (\alpha_3, 0)$ and $R^1_{0,1} = (\alpha_3, \alpha_3)$ are also states which live in the double core but not at weak coupling. These decay on the curves in figure 25.

10. The A_2 singularities

We have dealt with the the double cores which occur around the A_1 singularities of the singularity surface. There also exist two A_2 singularities at the critical radius $R = \sqrt{3}\Lambda$. Again the cores will coincide, and again we expect them to merge. That the coupling is strong in two root directions implies that it must be strong in the third root direction too. We do not expect a triple core. Therefore we must have three double cores squeezed up against each other in the neighbourhood of $R = \sqrt{3}\Lambda$ and $u = 0$. The fact that the right hand side of the α_i core always merges with the left hand side of the α_{i+1} core suggests how the three tubes slide through each other merging only pairwise, the detailed exposition of which this 2-dimensional medium does not lend itself.

Further decreasing the radius R now decreases the coupling strength slightly, although we still retain cores until just after the point when $R = \Lambda/\sqrt[6]{2}$ when the intersection with the singularity surface becomes empty. While $\Lambda/\sqrt[6]{2} < R < \Lambda\sqrt{3}$ we live in a region similar in many ways to when $\Lambda\sqrt{3} < R < \infty$, but, if anything, with a simpler structure. The branch cuts are shown in figure 27. Three toroidal cores exist around the quantum cuts. The G's all pass through the A_2 singularities, after which they 'untie' globally such that each G is rotationally symmetric about the centre of the torus around which it wraps, as shown in figure 28.

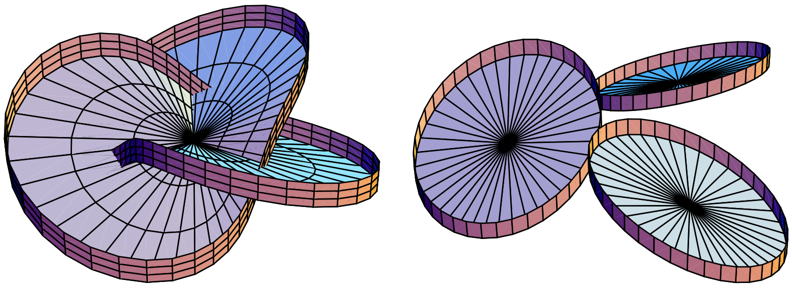

Figure 27: The branch cuts for large and for small radii.

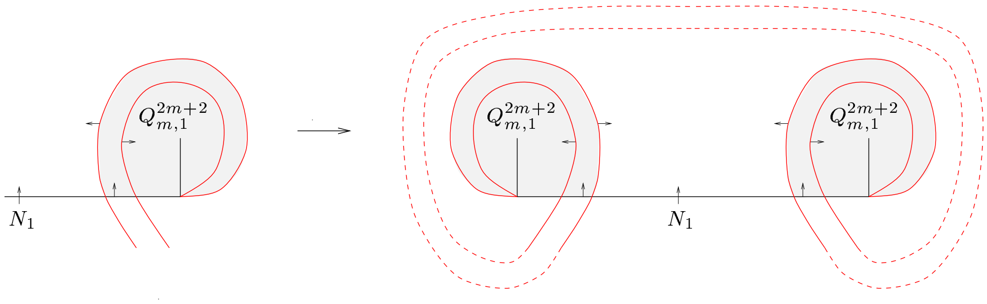

Figure 28: The local wrapping is mirrored in this sector.

11. Remarks

We have found a consistent model of the moduli space of pure SU(3) with no matter hypermultiplets, and seen that there are disjoint bounded regions called double cores within which there exist only a finite number of BPS states, all in the form of hyper- and vector multiplets. There are none of the three semiclassical gauge bosons in these regions, instead there exist states P_i with charges given by the difference of the charges of two of the gauge bosons.

Our analysis also predicts the existence semiclassically of $Q^n_{2m,2}$ and $Q^n_{2m,3-}$ with charges $(\alpha_1, (n-1)\alpha_1 + 2m\alpha_2)$ and $(\alpha_2, n\alpha_2 - 2m\alpha_3)$ respectively. We speculate that perhaps these are generated in a similar manner to the states $Q^n_{2m,1}$, whereby they can be seen as the effect of exciting momentum in the compact $\{\alpha_3 - (-\alpha_2)\}$ and $\{\alpha_3 - (-\alpha_1)\}$ directions respectively of a higher dimensional monopole moduli space with potential, a sort of Witten effect which vanishes upon alignment of the two Higgs vevs. These directions are precisely those of P_1 and P_2, and indeed we see towers created at strong coupling caused by excitation in these directions alone, with the charge proportional to the magnetic charge in units $\{0, \pm 1\}$ as for SU(2).

There is an alternative formulation of the BPS states as M2-branes in M-theory [16, 17, 18, 19] which may shed further light on this problem. Of particular interest is how a higher spin multiplet may be interpreted, and the number of boundaries it might possess, perhaps twice the value of the highest spin state in the multiplet.

There also exists an index theorem calculation of Stern and Yi [32] which counts the BPS states for SU(n). This gives a lower bound on the number of states present and could lead to a more definitive statement as to whether or not any of these new states occur. In [33] Lerche predicts the BPS spectrum at the point $u = v = 0$. We cannot reach this point in our model. This is because the stereographic projection we use in the quantum case gives the trefoils

$$\left| v \pm \frac{\Lambda^3}{2} \right|^2 = \left| u^{3/2} \mp \frac{\Lambda^3}{2} \right|^2 = \frac{2R^6 - \Lambda^6}{4},$$

subject to $|u|^3 + |v|^2 = R^6$.

Another interesting direction of further study would be to look at the case of SU(3) with 3 flavours of fundamental hypermultiplet. There is evidence that at certain points of this theory there is a correspondence to a particular 2-dimensional (2,2)-supersymmetric U(1) gauge theory with 3 flavours of twisted chiral multiplets [14, 15, 21]. This two dimensional theory has a strong-coupling expansion from which one can extract results about the four dimensional theory unobtainable by other means. Agreement with this correspondence would lend further weight to the veracity of both ideas.

Acknowledgments

We would like to thank Nick Dorey, Jerome Gauntlett, Tim Hollowood, Stephen Howes, David Olive, Peter West, and especially Dave Tong for useful conversations and suggestions.

References

[1] N. Seiberg and E. Witten, *Electric-magnetic duality, monopole condensation and confinement in $N = 2$ supersymmetric Yang-Mills theory*, *Nucl. Phys.* **B 426** (1994) 19 [hep-th/9407087].

[2] N. Seiberg and E. Witten, *Monopoles, duality and chiral symmetry breaking in $N = 2$ supersymmetric QCD*, *Nucl. Phys.* **B 431** (1994) 484 [hep-th/9408099].

[3] F. Ferrari and A. Bilal, *The strong-coupling spectrum of the Seiberg-Witten theory*, *Nucl. Phys.* **B 469** (1996) 387 [hep-th/9602082].

[4] A. Bilal and F. Ferrari, *Curves of marginal stability and weak and strong-coupling BPS spectra in $N = 2$ supersymmetric QCD*, *Nucl. Phys.* **B 480** (1996) 589 [hep-th/9605101].

[5] A. Bilal and F. Ferrari, *The BPS spectra and superconformal points in massive $N = 2$ supersymmetric QCD*, *Nucl. Phys.* **B 516** (1998) 175 [hep-th/9706145].

[6] F. Ferrari, *Charge fractionization in $N = 2$ supersymmetric QCD*, *Phys. Rev. Lett.* **78** (1997) 795 [hep-th/9609101].

[7] C. Fraser and T.J. Hollowood, *On the weak coupling spectrum of $N = 2$ supersymmetric* SU(N) *gauge theory*, *Nucl. Phys.* **B 490** (1997) 217 [hep-th/9610142].

[8] T.J. Hollowood, *Dyon electric charge and fermion fractionalization in $N = 2$ gauge theory*, *Nucl. Phys.* **B 517** (1998) 161 [hep-th/9705041].

[9] T.J. Hollowood, *Semi-classical decay of monopoles in $N = 2$ gauge theory*, hep-th/9611106.

[10] A. Klemm, W. Lerche and S. Theisen, *Nonperturbative effective actions of $N = 2$ supersymmetric gauge theories*, *Int. J. Mod. Phys.* **A 11** (1996) 1929 [hep-th/9505150].

[11] P.C. Argyres and M.R. Douglas, *New phenomena in* SU(3) *supersymmetric gauge theory*, *Nucl. Phys.* **B 448** (1995) 93 [hep-th/9505062].

[12] J.P. Gauntlett, N. Kim, J. Park and P. Yi, *Monopole dynamics and BPS dyons in $N = 2$ super-Yang-Mills theories*, *Phys. Rev.* **D 61** (2000) 125012 [hep-th/9912082].

[13] E. Witten, *Phases of $N = 2$ theories in two dimensions*, *Nucl. Phys.* **B 403** (1993) 159 [hep-th/9301042].

[14] A. Hanany and K. Hori, *Branes and $N = 2$ theories in two dimensions*, *Nucl. Phys.* **B 513** (1998) 119 [hep-th/9707192].

[15] N. Dorey, *The BPS spectra of two-dimensional supersymmetric gauge theories with twisted mass terms*, *J. High Energy Phys.* **11** (1998) 005 [hep-th/9806056].

[16] E. Witten, *Solutions of four-dimensional field theories via M-theory*, *Nucl. Phys.* **B 500** (1997) 3 [hep-th/9703166].

[17] M. Henningson and P. Yi, *Four-dimensional BPS-spectra via M-theory*, *Phys. Rev.* **D 57** (1998) 1291 [hep-th/9707251].

[18] A. Mikhailov, *BPS states and minimal surfaces*, *Nucl. Phys.* **B 533** (1998) 243 [hep-th/9708068].

[19] A. Fayyazuddin and M. Spalinski, *The Seiberg-Witten differential from M-theory*, *Nucl. Phys.* **B 508** (1997) 219 [hep-th/9706087].

[20] P.C. Argyres, M. Ronen Plesser, N. Seiberg and E. Witten, *New $N = 2$ superconformal field theories in four dimensions*, *Nucl. Phys.* **B 461** (1996) 71 [hep-th/9511154].

[21] N. Dorey, T. Hollowood and D. Tong, *The BPS spectra of gauge theories in two and four dimensions*, *J. High Energy Phys.* **05** (1999) 006 [hep-th/9902134]

[22] A. Klemm, W. Lerche and S. Theisen, *Nonperturbative effective actions of $N = 2$ supersymmetric gauge theories*, *Int. J. Mod. Phys.* **A 11** (1996) 1929 [hep-th/9505150].

[23] A. Hanany and Y. Oz, *On the quantum moduli space of vacua of $N = 2$ supersymmetric* $\mathrm{SU}(N_c)$ *gauge theories*, *Nucl. Phys.* **B 452** (1995) 283 [hep-th/9505075].

[24] A. Brandhuber and K. Landsteiner, *On the monodromies of $N = 2$ supersymmetric Yang-Mills theory with gauge group* $\mathrm{SO}(2N)$, *Phys. Lett.* **B 358** (1995) 73 [hep-th/9507008].

[25] U.H. Danielsson and B. Sundborg, *The moduli space and monodromies of $N = 2$ supersymmetric* $\mathrm{SO}(2r+1)$ *Yang-Mills theory*, *Phys. Lett.* **B 358** (1995) 273 [hep-th/9504102].

[26] P.C. Argyres and A.E. Faraggi, *The vacuum structure and spectrum of $N = 2$ supersymmetric* $\mathrm{SU}(N)$ *gauge theory*, *Phys. Rev. Lett.* **74** (1995) 3931 [hep-th/9411057].

[27] A. Klemm, W. Lerche, S. Yankielowicz and S. Theisen, *Simple singularities and $N = 2$ supersymmetric Yang-Mills theory*, *Phys. Lett.* **B 344** (1995) 169 [hep-th/9411048].

[28] P.C. Argyres and A.D. Shapere, *The vacuum structure of $N = 2$ superqcd with classical gauge groups*, *Nucl. Phys.* **B 461** (1996) 437 [hep-th/9509175].

[29] U.H. Danielsson and B. Sundborg, *Exceptional equivalences in $N = 2$ supersymmetric Yang-Mills theory*, *Phys. Lett.* **B 370** (1996) 83 [hep-th/9511180].

[30] M.R. Abolhasani, M. Alishahiha and A.M. Ghezelbash, *The moduli space and monodromies of the $N = 2$ supersymmetric Yang-Mills theory with any Lie gauge groups*, *Nucl. Phys.* **B 480** (1996) 279 [hep-th/9606043].

[31] C.N. Pope, *Axial vector anomalies and the index theorem in charged Schwarzschild and Taub-Nut spaces*, *Nucl. Phys.* **B 141** (1978) 432.

[32] M. Stern and P. Yi, *Counting Yang-Mills dyons with index theorems*, *Phys. Rev.* **D 62** (2000) 125006 [hep-th/0005275].

[33] W. Lerche, *On a boundary CFT description of nonperturbative $N = 2$ Yang-Mills theory*, hep-th/0006100.